Journal of The Electrochemical Society, **153** (2) G149-G159 (2006)
0013-4651/2006/153(2)/G149/11/$20.00 © The Electrochemical Society

Organic Airborne Molecular Contamination in Semiconductor Fabrication Clean Rooms

A Review

Walter Den,[a,z] Hsunling Bai,[b] and Yuhao Kang[b]

[a]*Department of Environmental Science and Engineering, Tunghai University, Taichung, 407 Taiwan*
[b]*Graduate Institute of Environmental Engineering, National Chiao Tung University, Hsinchu 300, Taiwan*

Monitoring of airborne molecular contamination (AMC) has become a crucial element of cleanroom management as the production phase of semiconductor devices marches deep into sub-100-nm range. The current understandings of the AMC, particularly those with organic origins, are presented comprehensively in this article based on the research reports within the past ten years. Starting with a review of the chronological development of AMC problems and several approaches for the AMC classifications, this article also examines the merits of several available ambient sampling and surface analytical methods. The focal point of the article is to address the surface deposition potential of organic AMCs by experimentally correlating the surface speciation and abundance of the organic AMCs with their physical and chemical characteristics, together with the kinetic models delineating the rates of deposition for both single-and multiple-contaminant scenarios. In addition, the current progress of the AMC control strategies, especially the development of the chemical filtration technology, is also examined in the paper.
© 2006 The Electrochemical Society. [DOI: 10.1149/1.2147286] All rights reserved.

Manuscript submitted July 7, 2005; revised manuscript received October 12, 2005. Available electronically January 4, 2006.

Cleanrooms, as one may expect, are designed in an attempt to maximize production rates and yields for environmentally sensitive materials (microelectronics and pharmaceutical elements or products), processes (wafer fabrication), or operations (medical procedures). However, only in the field of wafer fabrication processes are the concept of cleanrooms sufficiently uniform that comparison between the demands of air cleanliness becomes meaningful; hence, the discussion on the microcontamination is strictly focused on the semiconductor cleanroom environment. For many years, the degree of cleanliness refers to minimization of airborne particulates in cleanrooms to prevent formation of product defects. This requirement motivated the design classification of semiconductor cleanrooms into strictly particulate-defined environments, such as class 10 (ISO 4), class 100 (ISO 5) cleanrooms. Further restrictions on the temperature and humidity, pressure uniformity, airflow velocity and distribution, noise and vibration levels, as well as the electrostatic discharge control, have become the standard practices to establish critical environments for semiconductor device fabrication that meets the required product yield and reliability.

When the critical device geometry fell below a quarter micrometer range, however, the concept of particle-free environment no longer ensures product reliability. The transformation of "ballroom" type into "bayroom" type cleanrooms, coupled with the introduction of fan-filter unit (FFU) and standard mechanical interface (SMIF), is still driven to prevent particulate contamination to accommodate the advances of larger wafers (300 mm) and small feature sizes (subquartermicrometer). Despite these precautionary and sometimes expensive efforts, occasional and irregular deterioration of wafer characteristics were still experienced for unknown reasons, until the defects were spotted and linked with the facility environments. This type of microcontamination has been known as the airborne molecular contamination (AMC), which is a rather generic term because the contaminants may be in the form of gas, vapor, or even aerosols with vastly different chemical natures. Therefore, even though the control of these AMCs has been recognized as an essential design requirement for all new semiconductor manufacturing facilities, the complexity of the problem, such as the variation in the source and ambient concentration as well as the impacts on the fabrication process, largely hamper the development of an effective or standardized control strategy. For example, chemical filters targeting the removal of gaseous contaminants typically attain an efficiency of 99%. This efficiency is much less than the particulate-filter devices, which typically are capable of attaining 99.97% for particles larger than 0.3 μm (high-efficiency particle air filter, HEPA) and 99.999% for particles larger than 0.12 μm ultralow penetration air filter (ULPA). The requirements for the removal of AMCs, nevertheless, were not nearly as definitive as those for particulate control, primarily due to the lack of understanding of the degree of the AMC-induced damage on the fabrication processes.

In light of the growing significance of the potential problems associated with AMCs, this article intends to provide a comprehensive review of the current understanding of AMCs, including the approaches of their classification, as well as the source identification and the sampling methods of AMCs. This will be followed by a discussion on the adsorption potential of AMCs with organic links, which have been probed as the main culprit of many types of fabrication defects. Subsequently, the kinetic models having been developed in recent years to describe the rate of surface deposition for both single and multiple species are reviewed. The final section of the article is denoted to a delineation of several feasible control strategies, particularly to the state-of-the-art development of chemical filtration for the control of AMCs.

Chronology of AMCs

Definition and sources of AMCs.— AMC, in principle, is a generic term encompassing gaseous- or vapor-state pollutants from any part fugitive source or emission that are detrimental to any part of the wafer fabrication process. Typically with very low ambient concentrations (several parts per billion by volume), the ubiquitous presence of AMCs had been mostly ignored because their adverse effects on device fabrication were practically insignificant as compared to those caused by particle deposition. In fact, the issue of AMCs did not become a particular concern until the early 1990s, when the fabrication feature size marched into sub-half-micrometer ranges, that device breakdown problems stemming from the deposition of airborne contaminants were identified. Monitoring of the ambient air quality inside and outside the facilities was initially practiced in attempts to correlate the surrounding air with the gaseous compounds in the cleanrooms due to contamination of the supply air. Studies have revealed that unusually high concentrations of chlorine and boron were detected in cleanrooms for fabs located in the vicinity of coastal areas, and that the presence of ammonia and amines was closely linked to the fabs near agricultural activities using a high volume of alkaline fertilizers. In many cases, areas with significant semiconductor manufacturing activities are also those of advanced industrial cities, where poor ambient air qualities were frequently experienced due to heavy traffic. As a consequence, many volatile organic compounds (VOCs) with concentrations as high as a few parts-per-million have been identified in the cleanrooms. The

[z] E-mail: wden@mail.thu.edu.tw

Downloaded on 2014-04-26 to IP 140.113.38.11 address. Redistribution subject to ECS terms of use (see ecsdl.org/site/terms_use) unless CC License in place (see abstract).

problems associated with contamination from outside air can be effectively managed with the installation of high-efficiency chemical filters at the make-up air and recirculation air compartments. In addition, for processes requiring the highest levels of air cleanliness, the use of minienvironments, which are essentially independent of the external cleanroom air through optimization of the airflow and ventilation schemes, has become a popular choice.

Besides contamination of the air supply, a number of wafer fabrication processes themselves can be a major source of airborne contamination. An example of the process-induced microcontamination was brought up in a study by MacDonald and co-workers,[1,2] who investigated the deterioration of lithographic performance by organic vapor contamination. In those studies, exposure of wafers coated with a chemically amplified deep ultraviolet (DUV) resist, used to capture sub-0.3-μm images, in air containing less than 15 ppb organic base vapor severely degraded the image quality of the resist systems. These organic bases containing amines or ammonia functional groups permeated into the resist film and changed the quantum efficiency of the reaction at the resist–air interface, widening or distorting the trench on the top of the resist profile (i.e., T-top phenomenon). Incidentally, the organic base compounds could be found in many fabrication chemicals such as *N*-methyl pyrollidone (NMP) and tetramethyl ammonium hydroxide (TMAH), the major constituents widely used for resist coating and stripping. These results convey the importance of AMC control because the lithography-induced critical dimensions using chemically amplified photoresists essentially dictate the device characteristics in the 150-nm-technology node and possibly beyond,[3,4] and thus is a yield-limiting factor for the device fabrication line.

Identification of the process-induced AMC contamination spurred the endeavors to conduct real-time monitoring of air in different process areas. Areas of ion implantation are typically contaminated with arsine, boron, phosphine, and hydrochloric acid vapors, while trace concentrations of Freons, carbon tetrachloride, HCl, and HF are linked to the plasma etch tools. The potential impacts of the inorganic AMCs have also been implicated, as Lue et al.[5,6] presented evidence of gas-to-particle generation from SO_2 gas during vacuum pumpdown and venting. Corrosive gases such as HCl and HF could also lead to corrosion of metal interconnects or gradual degradation of production tools. The presence of boron and phosphate contamination is also a special concern as they could lead to unintentional p-type or n-type doping into doped layers.[7,8] Bai et al.[9] also demonstrated, through electron microscopic observation and elemental analysis of particles on the wafers exposed in the lithographic area of a cleanroom, that inorganic molecules including phosphate, sulfur, chlorine, and metallic elements may bind to condensed organic matter to form particulates as large as 50 μm in width. These findings and observations also entail that the extent of gaseous contamination does not necessarily correspond to that of particle contamination in cleanrooms. The contamination-sensitive processes located in a class 1 cleanroom typically involve a greater quantity of process-related chemicals; hence, the possibility of vapor emissions is also greater than the processes located in lower levels of cleanroom.

A wide range of organic volatile vapors has also been detected in process areas such as lithography and wet stations. Organic vapors are particularly problematic due to their abundance, greater mobility (e.g., diffusivity), and low vapor pressures. These characteristics render organic vapors to have faster surface deposition rates than particles and easily condense on the surface of wafers. Organic molecules depositing on wafer surfaces have been documented to cause several device performance deterioration mechanisms, such as increased surface roughness, formation of hazing and streaking, as well as damage of epitaxial growth.[10,11] The most notable effect, however, is perhaps the degradation of gate oxide integrity.[10,12,13] In particular, Tamaoki et al.[12] observed that the breakdown field strength of an interpolysilicon SiO_2 layer (i.e., Si substrate covered with a layer of thermal oxide and two layers of polysilicon) progressively reduced with longer exposure times. With no evidence of organic contamination in the polysilicon layers, they suspected that the contamination in the thermal oxide layer was responsible for the degradation of electrical characteristics. They also suggested that organic contamination should be less than 10 ng per 150-mm wafer using unstructured C_8H_{16} as the contaminant. Furthermore, Rana et al.[14-16] studied the effects of isopropanol (IPA) and butyl hydroxy toluene (BHT) on the quality of ultrathin gate oxides by thermal oxidation. They determined that the adsorption capacity and kinetics of polar organic molecules was highly dependent on the surface hydrophobicity (HF-last cleaned) or hydrophilicity (as-received), as BHT caused a larger number of carbon-based defects on the HF-cleaned wafers. These researchers also pointed out that the preadsorption of moisture plays an immense role in the adsorption and desorption of organic molecules such as IPA and BHT on the SiO_2 wafers, especially when high-temperature processes are involved to initiate adsorption with chemical bonding (i.e., chemisorption), such as Si–C bond formation. Incorporation of the carbon impurities caused high leakage currents due to direct tunneling for the oxides. Moreover, Kitajima and Shiramizu[17] demonstrated that the breakdown characteristics of the thin gate-oxide film were influenced by organic contaminants such as benzenoid with a hydrophilic group. They also determined that the device characteristics can be degraded if the organic density on a bare silicon surface exceeds approximately $1 \times 10^{13}\ cm^{-2}$ (as carbon).

Table I. AMC Classification proposed in SEMI F21-85.[18]

Classification	Concentration (pptM) 1	10	100	1000	10000
Acid	MA-1	MA-10	MA-100	MA-1000	MA-10000
Base	MB-1	MB-10	MB-100	MB-1000	MB-10000
Condensable	MC-1	MC-10	MC-100	MC-1000	MC-10000
Dopant	MD-1	MD-10	MD-100	MD-1000	MD-10000

Example of
Acids: HF, H_2SO_4, HCl, HNO_3, H_3PO_4, HBr.
Bases: NH_4OH, tetramethylammonium, tetramethyl amine, tetraethyl amine, *N*-methyl-pyrrolidinone, cyclohexylamine, diethylaminoethanol, methylamine, dimethylamine, ethanolamine.
Condensables: silicone, hydrocarbons, DOP, DBP, DEP, BHT.
Dopant: boron, organophosphates, arsenates, B_2H_6, BF_3, AsH_3, TEP, TCEP, TPP.

Classification of AMCs.— Given the recognition of the importance of AMCs, an initial set of industrial standards was produced by Semiconductor Equipment and Materials International (SEMI), known as the SEMI Standard F21-95.[18] This standard broadly classifies molecular contaminants into four groups, namely A(cids), B(ases), C(ondensables), and D(opants). This classification consists of an "M" nomenclature followed by a designated class letter and an integer that indicates the maximum allowable total concentration in parts-per-trillion molar (pptM), as exemplified in Table I. While SEMI F21-95 provides a general guideline to follow, it fails to distinguish the chemical category of many compounds, particularly those of organic nature. For instance, an organic molecule can be classified as either MA or MB, even though condensation may have been more important in its adverse effect to the fabrication process. Perhaps more significantly, the standard is flawed because it does not correlate AMC cleanliness to device yield or reliability. For this reason, the Semiconductor Industrial Association (SIA), with technical aid from Sematech, denoted an area in its published "International Technology Roadmap For Semiconductors" (ITRS) to present recommendations on process-specific requirements, including pre-gate oxidation, salicidation, contact formation, and DUV lithography (Table II). These criteria are based on groups of molecular contaminants as opposed to individual species to account for the possible synergistic effects between contaminants and surfaces.

Downloaded on 2014-04-26 to IP 140.113.38.11 address. Redistribution subject to ECS terms of use (see ecsdl.org/site/terms_use) unless CC License in place (see abstract).

Table II. Process-specific criteria of AMC limits.[67]

Years (Technology node, nm)	2001 (150)	2002 (130)	2003 (107)	2004 (90)	2005 (80)	2006 (70)	2007 (65)	2010 (50)	2013 (35)	2016 (25)
Lithography-base (as amine, NH_3)	750	750	750	750	750	<750	<750	<750	<750	<750
Gate-metal (as Cu)	0.2	0.2	0.15	0.1	0.1	0.07	<0.07	<0.07	<0.07	<0.07
Gate-organics (as Mw ≧ 250)	100	90	80	70	60	60	50	40	30	20
Contact acid (as Cl^-)	10	10	10	10	10	<10	<10	<10	<10	<10
Contact base (as NH_3)	20	16	12	10	8	4	<4	<4	<4	<4

A rather unique approach, namely, the method of reactivity monitoring, was proposed to characterize the destructive potential of an AMC-contaminated environment.[19,20] By employing measurement devices such as environmental reactivity coupons (ERCs) or quartz crystal microbalances (QCMs) containing test metal films such as copper and silver, the extent of metal-film corrosion as individual or total corrosion can be quantified and used as the basis of AMC control strategies. Table III provides an example of cleanroom classification based on the method of reactivity monitoring.

It is worth noting that due to the industry's competitiveness, individual semiconductor (including both microelectronics and optoelectronics) manufacturers tend to set their own contamination control criteria, which sometimes even become a proprietary item. Therefore, there is still no consensus criterion of AMC contamination control depending on the capability and expectation of the manufacturers. The range of variability, however, is expected to significantly narrow as the critical geometries converge to those forecasted by the ITRS.

Deposition of Organic AMCs (oAMCs) on Wafers

Sampling and analysis of oAMCs.— Sampling and analysis of volatile and semivolatile organic contaminants in air has been well established and standardized.[21,22] Gaseous-phase contaminants are easily extracted by sorption tubes packed with sorbents of either polymeric or carbonaceous materials, or a mixture thereof, to selectively retain compounds of different chemical natures such as hydrophobicity and polarity. The sampling tubes are then subjected to quantitative and qualitative analysis, most commonly by gas chromatography (GC) coupled with a mass spectrometer (MS). A number of researchers have applied similar methods for the analyses of indoor air and cleanroom air. For example, Otake et al.[23] demonstrated low detection limits using GC-MS for samples collected by charcoal tubes, followed by solvent (toluene) extraction and separation in sequence through ultrasonication and centrifugation. Toda et al.[24] also used the GC-MS technique to simultaneously determine the airborne concentration of several phosphate and phthalate esters in cleanrooms. They collected these organic contaminants by a silica-based cartridge, followed by solvent extraction with syringe-injected acetone for elution of target contaminants. These extraction procedures give remarkably low detection limits but could be overly elaborating and time-consuming in meeting the requirement of frequent analyses for monitoring purposes. Alternatively, GC-MS preceded by a single- or two-stage thermal desorption (TD-GC/MS), sometimes enhanced by a cryofocusing collection, is also frequently applied for the quantitative analysis.[22,25,26] Recently, Kang et al.[27] determined the concentrations of two short-chained dialkyl phthalate esters in cleanroom air and wafer box air by the TD-GC/MS procedure. They found that the use of a modified quasi vaporizer to introduce the target analytes into the polymeric-based sorbent beds in vapor phase tubes was suitable for the preparation of calibration standards. This method proved to be reliable and produced high analytical sensitivity while avoiding contamination due to solvent extraction procedures.

Surface concentration of organic contaminants is rather difficult to quantify, especially for monolayer adsorption on wafer surfaces. Although X-ray photoelectron spectrometry (XPS) and time-of-flight secondary ion mass spectrometry (TOF-SIMS) have been used for spot detection of the organic contamination of silicon wafer surfaces,[28-30] both methods require high-vacuum conditions under which the loss of volatile components of the samples could become significant, and neither method is capable of achieving full wafer analysis. Alternatively, the adsorbed organic molecules on surfaces can be thermally desorbed and swept into a sampling tube with a metered stream of carrier gas. Subsequently the sorption tube can be analyzed by TD-GC/MS. A number of well-designed surface emission cells have been reported, ranging from a free emission cavity (Fig. 1a),[31] a full-wafer oven chamber (Fig. 1b),[27] to a commercially manufactured infrared-heating vacuum chamber (Fig. 1c). This type of analytical technique has been accepted and issued as the industrial standard method for organic analysis of silicon wafer surfaces, including the American Society for Testing and Materials (ASTM F1982-99),[32] the Institute of Environmental Sciences and Technology (IEST WG-CC031),[33] and SEMI (SEMI E108-0301).[34] The setting of heating temperature is crucial to the application of thermal desorption of surface organic contaminants, because excessive heating not only thermally decomposes the parent contaminants but also induces unintended material outgassing from chamber components (e.g., O-rings, polymeric tubing) that may interfere with the interpretation of wafer outgassing tests.[27]

When assessing strategies for AMC monitoring and control, it is useful to understand the differences between evaluating contaminants that deposit on surfaces and those found in cleanroom air. Tamaoki et al.[12] discussed this issue when they identified the deposited molecules to be different from those detected by air-sampling methods. They noted that the major ambient VOCs such as toluene and aliphatic hydrocarbons hardly adsorbed on the wafers. In contrast, phthalic species such as dioctyl and dibutyl phthalates (DOP and DBP) tended to continually adsorb on wafers despite their low concentration in air. Kitajima and Shiramizu[17] further investigated the adsorptivity of DOP by heat-treating the DOP-contaminated wafers. They found that the C–O, C=O, and C–CHn bonds in DOP structure were unstable and easily vaporized from the surfaces.

Table III. Cleanroom classification based on material corrosivity.[19]

Copper reactivity			Silver reactivity		
Class	Air quality	Reactivity rate	Class	Air quality	Reactivity rate
C1	Pure	<90 Å/30 days	S1	Pure	<40 Å/30 days
C2	Clean	<150 Å/30 days	S2	Clean	<100 Å/30 days
C3	Moderate	<250 Å/30 days	S3	Moderate	<200 Å/30 days
C4	Harsh	<350 Å/30 days	S4	Harsh	<300 Å/30 days
C5	Severe	>350 Å/30 days	S5	Severe	>300 Å/30 days

Downloaded on 2014-04-26 to IP 140.113.38.11 address. Redistribution subject to ECS terms of use (see ecsdl.org/site/terms_use) unless CC License in place (see abstract).

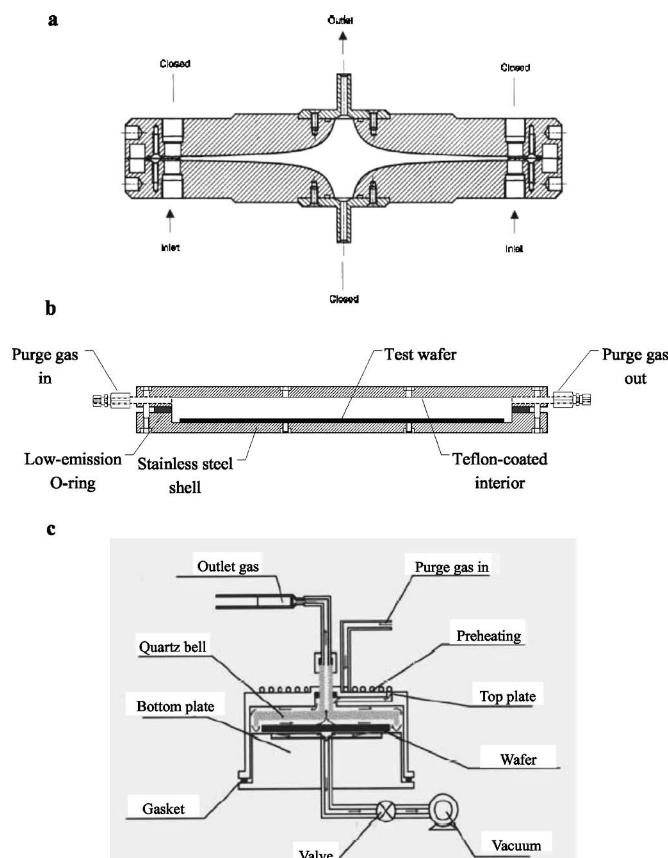

Figure 1. (a) Field and laboratory emission cell (after Ref. 25), (b) heat desorption chamber (after Ref. 27), and (c) wafer outgassing system (WOS, reproduced from Cascade Scientific, UK).

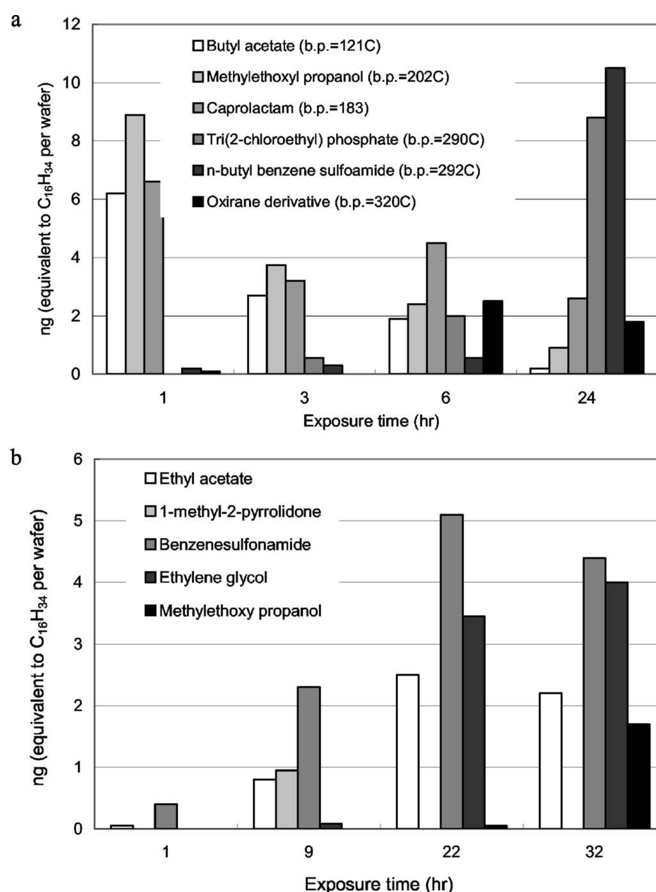

Figure 2. Evolution of surface organic species and quantities for (a) wafers exposed in cleanroom and (b) wafers stored in plastic boxes (after Ref. 35).

C=C bonds, however, were relatively stable and may decompose into C–C bonds. Moreover, Goodman et al.[30] utilized TOF-SIMS to track the surface concentration and species on wafers and observed rapid deposition of organic amines and amino alcohols in the initial days of exposure, particularly for the low-molecular-weight species. The surface amount of these nitrogen-containing molecules then gradually decreased over the next few months. In contrast, molecules such as DOP and polydimethylsiloxane (PDMS) showed continually increasing deposition for the first month and slowly leveled off.

Adsorption potential of oAMCs.— To examine the factors determining the surface affinity of the organic compounds, Sugimoto and Okamura[35] conducted extensive surface analyses of organic contaminants for wafers exposed in cleanroom environments and in plastic storage boxes. In their chromatographic analyses, a well-behaved relationship between the boiling point of the organic compounds and the retention time in the analytical column was obtained; therefore, a definitive boiling point could be assigned to an uncharacterized organic contaminant detected on the wafer surfaces. As shown in Fig. 2a, by tracking the time-dependent surface mass of six organic compounds with boiling points ranging between 121 and 320°C for wafers exposed in cleanroom ambience up to 24 h, they observed that organic contaminants with low boiling points tended to be adsorbed immediately. These contaminants, however, continually decreased with exposure time and were gradually replaced by organic contaminants with higher boiling points, indicating that vaporization activity of the organic contaminants was the decisive factor of their adsorption behavior. On the contrary, when wafers were stored in plastic boxes, they were exposed to organic contaminants with a much narrower range of boiling points. Unlike the previous case, they did not find a clear relationship between the storage time and the boiling points with respect to the amount of surface contaminants. Rather, they noted that organic contaminants bearing –C=O or –S=O functional groups tended to be adsorbed on wafer surfaces within 2 days of storage, whereas those having –O– groups were not detected until nearly 10 days (Fig. 2b). This result manifested that the degree of polarity of the contaminants in relation to the surface also plays a critical role to the adsorption of organic molecules.

Similarly, the preparation of surface coating is also important to the adsorption potential of oAMCs. Silicon wafers covered with insulating films such as SiO_2 and Si_3N_4 tend to favor adsorption of organic molecules containing polar functional groups such as –C=O, =NH, $-NH_2$. Conducting their studies in a well-controlled wafer exposure chamber, Kang et al.[36] have directly verified that SiO_2-coated wafer surfaces favored adsorption of diethyl phthalate (DEP) over Si_3N_4-coated surfaces after 4-h exposure, as shown in Fig. 3a. The differences in the surface deposition for the two types of wafer surfaces are related to the presence of the molecule-surface interacting forces. The intensity of polarity for the two types of wafer surfaces can be evaluated by the difference in the electronegativity ($\Delta\varepsilon$) between two bonding elements (i.e., Si–O and Si–N). In brief, electronegativity is a measure of the net tendency of a bonded atom in a molecule to attract electrons. The greater the difference in electronegativity of the two bonding elements, the more polar is the covalent bond with the more electronegative element bearing the partial negative charge. In this case, polarity of the SiO_2 thin film ($\Delta\varepsilon = 1.7$) is substantially greater than that of the Si_3N_4 thin film ($\Delta\varepsilon = 1.2$); hence, the DEP molecules tend to favor adsorption onto the wafers coated with SiO_2 thin film. Furthermore, Fig. 3b shows that DBP, a more polar compound than DEP by virtue

Downloaded on 2014-04-26 to IP 140.113.38.11 address. Redistribution subject to ECS terms of use (see ecsdl.org/site/terms_use) unless CC License in place (see abstract).

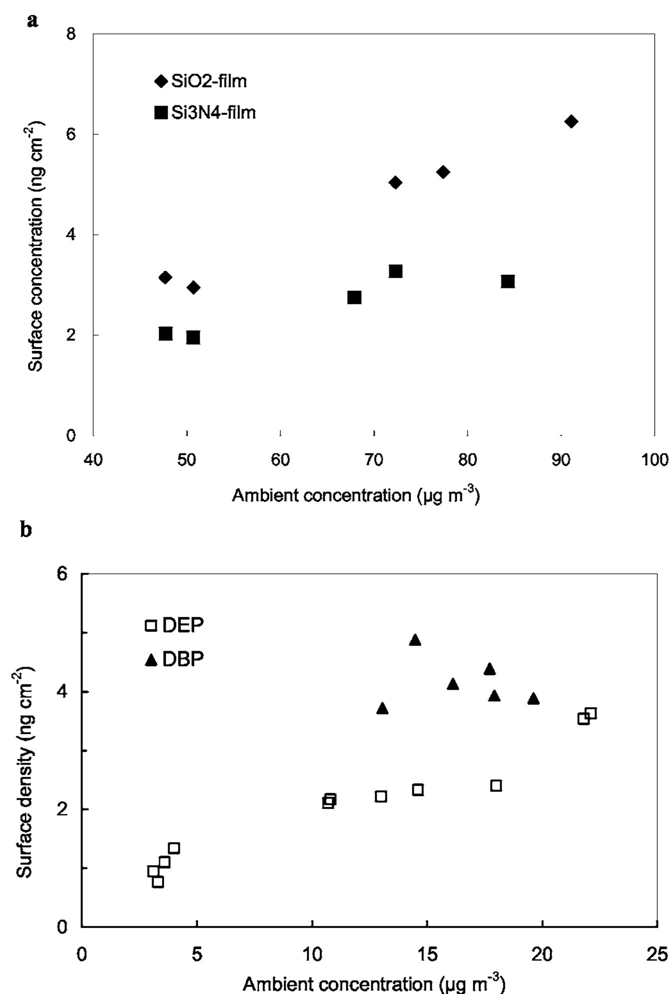

Figure 3. Surface concentration profiles for (a) 4-h exposure of DEP for wafers coated with SiO_2 and Si_3N_4 thin films (after Ref. 36), and (b) 4-h exposure of DEP and DBP for SiO_2 wafer (after Ref. 68).

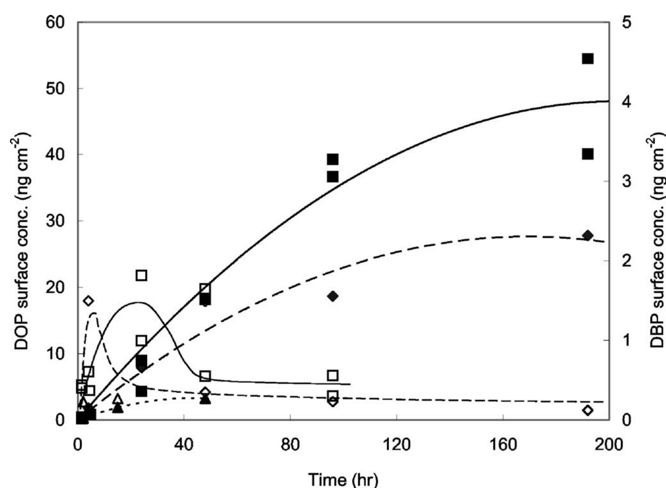

Figure 4. Surface concentration evolution of DOP [(■) Ref. 53; (◆, ▲) Ref. 50] and DBP [(□) Ref. 53; (◇, △) Ref. 50].

of its longer dialkyl chain, was more strongly adsorbed in the SiO_2-filmed wafer. One should be aware that organic molecules commonly include hydrophobic groups (e.g., $-CHn$); wafer surfaces covered with these molecules are more hydrophobic, causing decrease in the surface reaction efficiency in the fabrication process.

The stronger adsorption potential of phthalic and siloxane molecules over other more volatile oAMCs causes particular concern with respect to the control strategy of organic contaminants. While most oAMCs in cleanrooms originate from the supply air or process-related emissions, both phthalates and siloxanes are known to outgas from many polymeric surfaces and construction materials. In fact, DOP and its structural homologues (DBP, DEP, etc.) are common plasticizers used in wide variety of polymeric materials, and PDMS is a major constituent of silicone sealants. These compounds generally exhibit high molecular weights and high boiling points and are very stable once deposited onto wafer surfaces. Inoue et al.[37] reported the time-dependent variation of trace organic contamination detected in a newly constructed cleanroom. Among a range of organic species identified, they found that the presence of alkyl phthalic esters was persistent in the cleanroom over the first fifteen months before their ambient concentrations gradually decreased. Takeda et al.[38] further formulated the outgassing rate as a function of vapor pressure and ambient temperature for organic compounds from cleanroom construction materials. Figure 4 presents the surface density of DBP and DOP as a function of time for silicon wafers exposed in actual cleanrooms. All of these studies suggest that DOP becomes a prevailing organic contaminant for long-term exposure (>2 days), even though the surface abundance of DBP and other compounds was greater than DOP during the initial exposure period.

Perhaps the more significant issue arising from the favorable surface deposition of the phthalic compounds is the inevitable organic contamination of clean wafers stored in plastic wafer boxes,[39,40] presenting a problem which cannot be easily resolved by simply enhancing the air quality of the supply air through sophisticated chemical filters. For this reason, researchers have proposed a number of schemes to reduce the possibility of molecular contamination during wafer storage and handling. For instance, a closed system in which wafer transferring between any two processes is free from exposure to the cleanroom air was proposed by Ishihara et al.[41] The system is equipped with a clean dry air production unit through a series of catalysis and temperature-varied adsorption for circulation of purified air. At a smaller scale, the wafer pods can be purged by highly purified gas, typically by nitrogen of purity over 99.999%.[42,43] New fabs designed for 300-mm wafers are particularly adapted to purging as wafers are transported and stored in front opening unified pods (FOUPs)—a wafer boxed specially designed for automated transferring of large wafers. There appeared to be some controversy, however, on the optimization of the purging conditions. Veillerot et al.[44] found that continuous purging actually resulted in the worst electrical characteristics of gate-oxide among the tested purging conditions. In contrast, optimization of material outgassing, such as the use of silica-coated polycarbonate material, could be more effective for the prevention of organic outgassing and contamination.

Deposition kinetics.— Recognizing the potential degradation of device fabrication in the presence of phthalic compounds in cleanrooms, several research groups have been investigating the deposition kinetics of phthalic esters on the silicon wafers. In principal, when vapor-phase molecules arrive within a few atomic distances of the target surface in stagnant air, they are invariably attracted to the surface by the van der Waals force, especially for compounds with strong dipole moments. A portion of the molecules striking the surface may still possess sufficient residual energy to instantaneously rebound from the surface. Other less energetic molecules may remain on the surface for an extended period of time via physisorption, which is generally considered as an equilibrium process between adsorption and desorption occurring simultaneously. High gas-phase concentrations of contaminant typically favor adsorption to increase the amount of surface-bound molecules, whereas lower concentrations initiate desorption from the surface. Consequently,

Downloaded on 2014-04-26 to IP 140.113.38.11 address. Redistribution subject to ECS terms of use (see ecsdl.org/site/terms_use) unless CC License in place (see abstract).

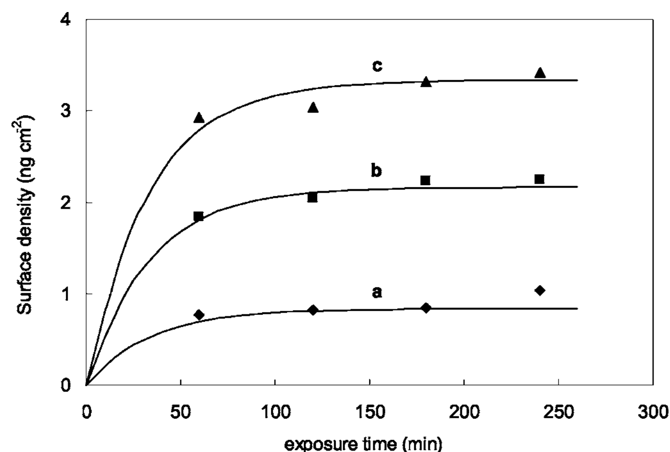

Figure 5. Experimental and predicted surface DEP concentration profiles for (a) $C_g = 5\ \mu g\ m^{-3}$; (b) $C_g = 13\ \mu g\ m^{-3}$; and (c) $C_g = 20\ \mu g\ m^{-3}$. The kinetic parameters used for model prediction are $k_{ads} = 3.7 \times 10^{-4}\ m^3\ \mu g^{-1}\ min^{-1}$ and $k_{des} = 0.03\ min^{-1}$ (after Ref. 36).

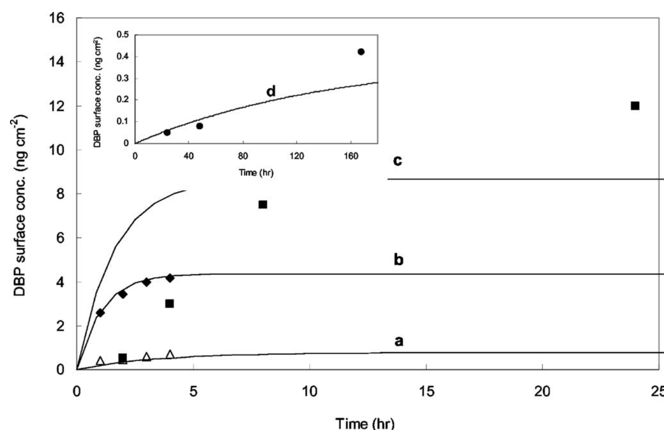

Figure 6. Experimental and predicted surface DBP concentration profiles. Data source: (△, ◆) Ref. 68; (■) Ref. 72; and (●) Ref. 73. The kinetic parameters used for model prediction are $k_{ads} = 3 \times 10^{-4}\ m^3\ \mu g^{-1}\ min^{-1}$, $k_{des} = 0.011\ min^{-1}$, and $C_{max} = 60\ ng\ cm^{-2}$ for (a) $C_g = 2\ \mu g\ m^{-3}$; (b) $C_g = 15\ \mu g\ m^{-3}$; (c) $C_g = 50\ \mu g\ m^{-3}$; and (d) $C_g = 0.1\ \mu g\ m^{-3}$.

the concentration gradient across the surface interface effectively dictates the rate of concentration equilibrium on the surface. To delineate the rates of change in the surface density, Zhu[45,46] proposed a generic surface kinetic model consisting of adsorption and desorption kinetics of first-orders

$$\frac{\partial C_s}{\partial t} = k_{ads}C_g - k_{des}C_s \qquad [1]$$

where C_s represents the surface density (ng cm^{-2}), C_g is the ambient concentration (μg m^{-3}), t is exposure time (min), k_{ads} and k_{des} are the adsorption rate constant (cm min^{-1}) and desorption rate constant (min^{-1}), respectively. The model assumed that the rate of adsorption is proportional to the molecular impingment flux, and that the rate of desorption follows the transition state theory, involving a potential energy well for a molecule to remain on the surface. This potential well could be calculated from a molecule-surface potential function described by a pair-wise sum of Lennard–Jones potentials. Solving for Eq. 1, one obtains

$$C_s(t) = C_g\left(\frac{k_{ads}}{k_{des}}\right)[1 - e^{-k_{des}\cdot t}] \qquad [2]$$

Based on Eq. 2, Kang et al.[36] attempted to quantify the rates of adsorption and desorption from a series of experiments using DEP as the model contaminant. As shown in Fig. 5, the results demonstrated that the surface densities of the SiO_2-coated wafers exposed under various ambient DEP concentrations ranging from 5 to 20 μg m^{-3} approached equilibriums within 4 h. By employing a combination of a simple trial-and-error method and a heuristic algorithm, the optimum values of the adsorption rate constant ($k_{ads} = 2.3 \times 10^{-3}$ cm min^{-1}) and desorption rate constant ($k_{des} = 1.9 \times 10^{-2}$ min^{-1}) were computed based on the best-fit curves between the calculated and experimental profiles. Although this model correctly depicts the surface deposition kinetics from low ambient concentrations and short exposure periods, its applicability is limited by failing to consider an adsorption ceiling. This limitation has been observed when the ambient DEP concentration was greater than 100 μg m^{-3}, resulting in a surface DEP density fluctuating at about 12 ng cm^{-2}. As a consequence, the model would overpredict the surface density when, in reality, no significant adsorption would occur after the surface adsorption sites are saturated.

To account for the limiting adsorption sites on a wafer surface, Eq. 1 can be modified into a Langmuir-type expression

$$\frac{\partial \theta}{\partial t} = (1 - \theta)k_{ads}C_g - k_{des}\theta \qquad [3]$$

where θ is the fraction of surface occupied by organic molecules. Alternatively, θ can be substituted by the surface density (C_s) to form another expression

$$\frac{\partial C_s}{\partial t} = (C_{s,max} - C_s)k_{ads}C_g - k_{des}C_s \qquad [4]$$

where $C_{s,max}$ represents the maximum surface adsorption capacity. The analytical solution of Eq. 4 is

$$C_s(t) = \left(\frac{C_{s,max}k_{ads}C_g}{k_{ads}C_g + k_{des}}\right)[1 - e^{-(k_{ads}C_g+k_{des})\cdot t}] \qquad [5]$$

Both Eq. 3 and 4 are valid for physisorption processes with strictly monolayer coverage, implying that adsorption of the impinging molecules will not occur once the surface adsorption sites are depleted. This phenomenon has been previously justified by Takahagi et al.,[47] who analyzed the surface carbon atomic ratio (C/Si) of as-received wafers by XPS. They concluded that the amount of carbon contamination on the wafers corresponded to an average film thickness of about 0.2 nm that conformed to the size of a molecule, and thereby warranting the existence of monolayer adsorption and a threshold surface organic capacity. Figure 6 shows the model predicted profiles along with the surface DBP density data obtained from literature as well as our own study. Using the kinetic parameters determined from this study (profiles a and b), the model satisfactorily predicts the realistic time-dependent DBP surface densities (profiles c and d) reported by other investigators. It was noted that the model tended to overpredict the short-term surface density but underpredict the long-term one, discrepancies that could be attributed to many factors such as the varying ambient DBP concentrations in the cleanrooms and the presence of other competing organic contaminants.

Realistically, wafers exposed in cleanroom environments or storage units are susceptible to a mixture of organic vapors. Some organic species will rapidly adsorb on the wafer surfaces, but they may gradually be replaced by other species with much stronger surface affinity, as exemplified in Fig. 2 and 3. Such time-dependent variation of surface adsorption species is known as the "fruit basket phenomenon," which usually occurs for long exposure periods (several weeks) as the surface adsorption sites are saturated. To mathematically describe this competitive surface organic kinetics between organic species with different chemical properties, Habuka

Downloaded on 2014-04-26 to IP 140.113.38.11 address. Redistribution subject to ECS terms of use (see ecsdl.org/site/terms_use) unless CC License in place (see abstract).

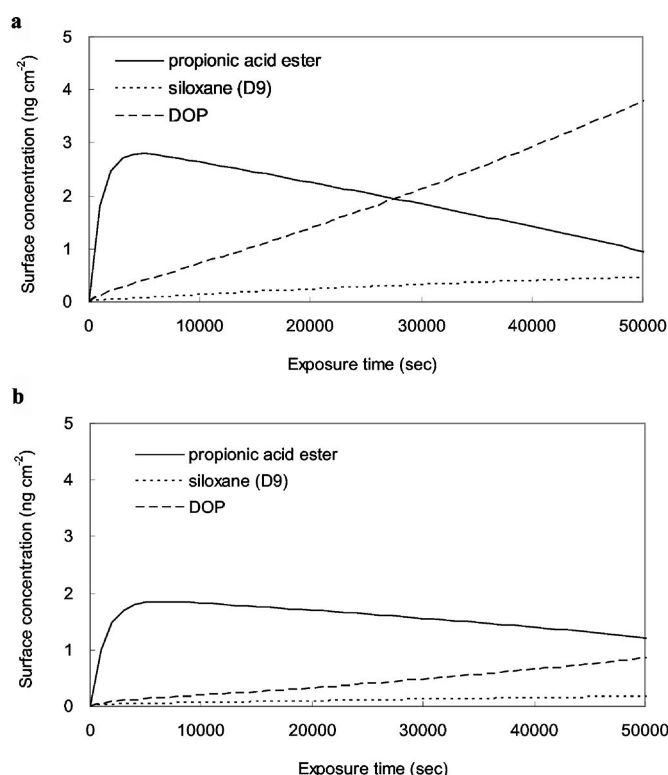

Figure 7. Simulative profiles for multicomponent deposition using the MOSAIC model (after Ref. 48) with the following kinetic parameters: (See Table IV

and co-workers[48,49] have developed a multicomponent organic species adsorption-induced contamination (MOSAIC) model by expanding Eq. 4

$$\frac{\partial C_{s,i}}{\partial t} = (C_{s,\max} - C_s)k_{\text{ads},i}C_{g,i} - k_{\text{des},i}C_{s,i} \quad [6]$$

where the sub-index i indicates the concentration of an individual organic species. The total organic density adsorbed on a wafer surface, therefore, is simply the mass-base sum of each individual species in addition to the pre-existing organic residue ($C_{s,bg}$)

$$C_s = \sum_j C_{s,j} + C_{s,bg} \quad [7]$$

where the sub-index j ($j \neq i$) refers to other organic species which could influence the surface density of species i. Defining the effective surface density as the difference between the maximum surface organic capacity and the background organic density

$$C_{s,e} = C_{s,\max} - C_{s,bg} \quad [8]$$

Eq. 6 then becomes

$$\frac{\partial C_{s,i}}{\partial t} = \left(C_{s,e} - \sum_j C_{s,j}\right)k_{\text{ads},i}C_{g,i} - k_{\text{des},i}C_{s,i} \quad [9]$$

Consequently, the increase in the surface density of organic species j would decrease the availability of sorption sites (i.e., the value of $C_{s,e}$-$\Sigma C_{s,j}$), causing reduction in the rate of adsorption of species i, $\partial C_{s,i}/\partial t$.

This model was validated using the actual data of wafer surface contamination by a three-component system (DOP/propionic acid ester/siloxane),[48] as illustrated in Fig. 7 for two types of wafer surface preparation. A more complex system composed of nine organic species has also been reported.[49] In both scenarios, the rate parameters $k_{\text{ads},i}C_{g,i}$, $k_{\text{des},i}$, and $C_{s,e}$ were determined for each organic species via a best-fit curve between the measured and the numerically calculated values at a specific exposure time. $k_{\text{ads},i}C_{g,i}$ values are estimated in conjunction because the ambient concentrations of organic species are often lacking or inconsistent. For limiting cases where the $C_{g,i}$ values are known, then $k_{\text{ads},i}$ may be determined as an individual parameter.[50] In these studies, the investigators observed three groups of organic species with distinct surface adsorption patterns, namely (I) those whose surface densities increase rapidly at the initial stage but decrease to a smaller density than their peak values, (II) those that increase rapidly initially and maintain their surface density near their peak values, and (III) those that increase gradually and continuously. In principle, the parameter $k_{\text{ads}}C_g$ determines the extent of initial surface adsorption and the parameter k_{des} dictates the surface affinity of an organic species. For example, an organic species of type (I) would exhibit relatively large values of both k_{ads} and k_{des}, whereas those of type (III) possess much smaller values of k_{des}. The values of the kinetic parameters for several dialkyl phthalates are summarized in Table V.

Table IV. (See Fig. 7)

Compound	$k_{\text{ads}}C$ (s^{-1})	k_{des} (s^{-1})	$S_{\max}$ (ng cm^{-2})
(a) UV–O_3 treated SiO_2 surface			
Propionic acid ester	3×10^{-4}	6×10^{-4}	
Siloxane (D9)	4×10^{-6}	0	6.0
DOP	2×10^{-5}	0	
(b) HF-cleaned Si wafer surface			
Propionic acid ester	4×10^{-4}	5×10^{-4}	
Siloxane (D9)	7×10^{-6}	4×10^{-6}	2.5
DOP	2×10^{-5}	0	

Surface adsorption capacity.— The surface adsorption capacity ($C_{s,\max}$) has a significant influence on the kinetic parameters, thus presenting a difficulty to the applicability of the models because much presumptive work has been involved in the process of determining its values due to the lack of experimental data. A starting method for estimating $C_{s,\max}$ is to calculate the mean molecular size of the target compound(s) using either van der Waals molecular volume increments[51] or the sophisticated molecular mechanics with stable molecular conformation.[52] Both methods produce similar values of projected molecular area for DEP (0.48 nm^2), DBP (0.59 nm^2), and DOP (0.77 nm^2). These values correspond to number densities of 2.1×10^{14}, 1.7×10^{14}, and 1.3×10^{14} molecules cm^{-2}, or mass densities of 58, 59, and 63 ng cm^{-2} for DEP, DBP, and DOP, respectively. Habuka and coworkers have calculated $C_{s,\max}$ by relating the peak density of an organic species with its steady-state density using Eq. 9 and have documented a broad range of values from 2.5 ng cm^{-2}[49] to as large as 54 ng cm^{-2}[53] for studies using different types of surface termination and organic species (Table VI). Okamura et al.[54,55] further dis-

Table V. Published values of deposition rate parameters for the dialkane phthalates.

	Adsorption			Desorption	
Species	k_a (m^3 μg^{-1} s^{-1})	C_g (μg m^{-3})	k_aC_g (s^{-1})	k_d (s^{-1})	Reference
DOP	⋯		2×10^{-5}	0	48
DBP	8×10^{-9}	0.1–2.8	⋯	4×10^{-6}	50
DOP	9×10^{-6}	0.12–0.6		0	
DEP	⋯		3×10^{-5}	3×10^{-2}	49
DBP			4×10^{-5}	7×10^{-4}	
DOP			3×10^{-5}	1×10^{-7}	
DEP	6.2×10^{-6}	5–100	⋯	5×10^{-3}	68
DBP	4.3×10^{-6}	2–15		1.8×10^{-4}	

Downloaded on 2014-04-26 to IP 140.113.38.11 address. Redistribution subject to ECS terms of use (see ecsdl.org/site/terms_use) unless CC License in place (see abstract).

Table VI. Published values of surface adsorption capacity.

Test compound(s)	S_{max} (ng cm^{-2})	Method of determination	Reference
DOP siloxanes (D9) propionic acid esters	2.5–6.0	Least-squares fitting with MOSAIC model	48
DEP DBP DOP	10		49
DBP DOP	28		50
DBP DOP Alkanoic acid esters	54		53
DBP	36–48	QCM	54 and 55
DEP DBP	78	Molecular volume computation	68

cussed the issue by employing the QCM method, which measures in real-time the weight differential between a dummy chamber and an adsorption chamber. They reported, using DBP as the test compound, that the saturate surface densities were 48 ng cm^{-2} for a "conventional" SiO_2-filmed surface and 36 ng cm^{-2} for a "polished" one. Evidently, the surface condition bears great significance on the surface adsorption capacity. For example, the sketch in Fig. 8 delineates the various possibilities of surface sorption sites, including (I) monolayer surface sites, (II) surface defects or atomic terraces, and (III) surface cavities. While all three types of surface sites are equally functional for deposition, molecular desorption from the monolayer sites is energetically much easier than those from surface defects and cavities. Therefore, unpolished or microscopically rough surfaces provide a larger number of total sorption sites than uniform surfaces; however, the sites belonging to types (II) and (III) may not be available because the molecules occupying those sites barely desorb. Considering that surface adsorption capacity is highly surface-sensitive, the values compiled in Table VI appear to be reasonably consistent, as they all fall in the same order of magnitude.

Sticking coefficients.— Besides the kinetic studies, quantification of the "sticking coefficients" (S_c) of the organic contaminants has also been proposed as a method to evaluate their propensity of surface deposition.[56,57] In a first approximation, the sticking coefficient of an organic species at steady-state conditions can be expressed as

$$S_c = \frac{C_s}{Jt} \quad [10]$$

where J denotes the mass impingment flux (g cm^{-2} s^{-1}). Under stagnant air, the mass impingment flux can be approximated by av-

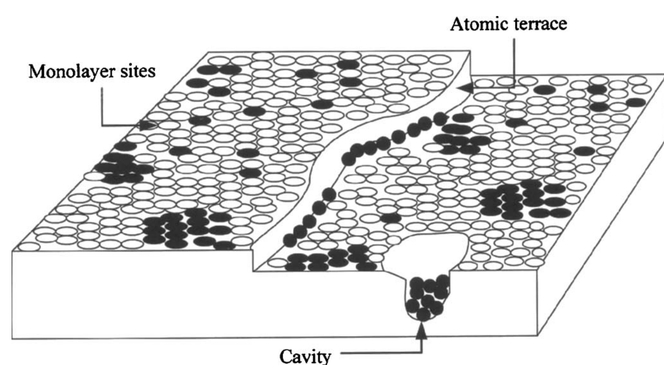

Figure 8. Schematics of surface sorption sites: (I) monolayer sorption sites, (II) surface defect or atomic terrace, (III) surface cavity (after Ref. 54).

Table VII. Published values of sticking coefficients.

Flow consideration	Test compounds	Sticking coefficient	Reference
Molecular flux only	DEP	3.0×10^{-6}	49
	DBP	1.7×10^{-4}	
	DOP	2.0×10^{-5}	
	TCEP[a]	9.5×10^{-6}	
	BHT[b]	6.5×10^{-7}	
	Siloxane (D10)	9.5×10^{-5}	
	DBP	7.8×10^{-5}	69
	DOP	3.4×10^{-5}	
	DEP (0–1 h)	2.4×10^{-6}	68
	DEP (0–4 h)	7.6×10^{-7}	
	DBP (0–1 h)	3.5×10^{-6}	
	DBP (0–4 h)	1.4×10^{-6}	
External flow field (vertical laminar flow)	DOP	2×10^{-3}	70
	Siloxanes (D3–D6)	$<1 \times 10^{-4}$	
	Aromatics	$<1 \times 10^{-5}$	
	DOP	7×10^{-3}	71
	TCEP[a]	7×10^{-3}	
	Siloxanes (D3–D6)	3×10^{-5}	
	DEP	$(6.7 \pm 2.8) \times 10^{-5}$	57 Laminar air flow 0.44 m s^{-1}
	DBP	$(8.9 \pm 2.7) \times 10^{-5}$	
	2-Ethyl 1-hexanol	$(9.2 \pm 4.1) \times 10^{-5}$	
	Phthalic anhydride	$(3.1 \pm 1.0) \times 10^{-3}$	
	Tetradecane	$(2.1 \pm 1.5) \times 10^{-3}$	
	Pentadecane	$(2.1 \pm 1.0) \times 10^{-3}$	
	TXIB[c]	$(1.2 \pm 0.5) \times 10^{-3}$	
	DMPP[d]	$(5.4 \pm 2.8) \times 10^{-4}$	

[a] Tris (2-chloroethyl) phosphate.
[b] 2,6-Di-*tert*-butyl-p-cresol.
[c] 2,2,4-trimethyl-1,3-pentanediol diisobutyrate.
[d] Dimethylpropylphthalate.

eraging over the Maxwell–Boltzmann distribution of molecular speed ($\bar{u}$) in the direction normal to the surface

$$J = \frac{1}{4} C_g \bar{u} \quad [11]$$

such that S_c may be rewritten as

$$S_c = \frac{C_S}{tC_g \frac{\bar{u}}{4}} \quad [12]$$

Under laminar flow, molecular movement is dominated by the external flow field, therefore Eq. 12 becomes

$$S_c = \frac{C_S}{C_g V t} \quad [13]$$

where V is the constant vertical laminar-flow velocity. Veillerot et al.[57] utilized Eq. 13 to perform linear regression analyses between the measured C_s values and the exposure time, and compiled the computer S_c values for eight identifiable organic compounds on Si and SiO_2 surfaces. These values ranged anywhere between 10^{-3} and 10^{-5}. Table VII summarizes the values of sticking coefficient from several studies. In general, the values of S_c under laminar flow are greater than those under stagnant air due to the convective transport rather than diffusive transport of molecules.

Despite its importance in film deposition theory, one is not advised to view the sticking coefficient as a kinetic parameter but rather as an indicator at best. Theoretically, S_c is merely a probabilistic term depicting the fraction of organic molecules to adsorb on the surface upon contact and is strongly dependent on the surface availability. Therefore, S_c is at maximum when a wafer surface is free of contamination and progressively decreases as the surface coverage increases. This condition could be further enlightened by

Downloaded on 2014-04-26 to IP 140.113.38.11 address. Redistribution subject to ECS terms of use (see ecsdl.org/site/terms_use) unless CC License in place (see abstract).

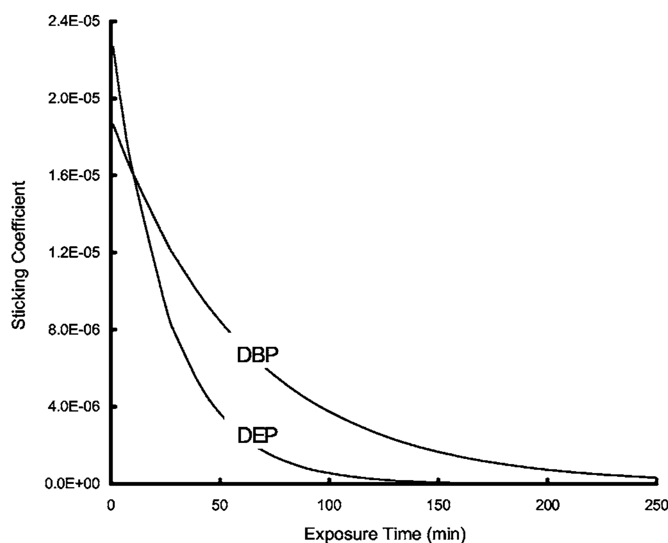

Figure 9. Time-dependent sticking coefficient for DEP and DBP calculated from their kinetic constants ($Cg = 20\ \mu g\ m^{-3}$).[68]

considering the last term of Eq. 5 (i.e., $e^{-(k_{ads}C_g+k_{des})t}$) as an equivalent of the time-dependent function of the sticking coefficient, revealing that S_c asymptotically approaches zero with time, as exemplified in Fig. 9. Therefore, S_c is much less definitive than the kinetic constants, although the values are informative with reference to the relative surface adsorptivity of the organic contaminants under the same exposure conditions. On the contrary, the values in Table VII should not be compared between difference studies, even for the same compound, because they may not be evaluated in the same time frame.

Control of oAMC Contamination

The current state of control technology and strategy for the minimization of oAMC problems can be broadly divided into three categories, namely, (*i*) outgassing source monitoring and control, (*ii*) isolation of wafer processing environment, and (*iii*) elimination of AMC in the processing environment through installation of chemical filters. Saito[58] compared the oAMC contamination using different control strategies, and observed that the utilization of chemical filtration in the processing environments (e.g., cleanroom make-up and/or recirculation air ventilation, fan-filter units, minienvironment, etc.) yielded the least-contaminated wafer surface based on the GC/MS analyses, followed by air replacement with ultrapure nitrogen gas, which is still a typical practice in the state-of-the-art FOUP systems for wafer isolation. The worst method was to simply store the wafers in plastic containers due to surface outgassing as previously described. In fact, several key materials, which are necessary for cost-effective cleanroom construction, equipment fabrication, or device assembly, are intrinsically sources of contamination. Examples range from the well-recognized construction material outgassing (floor tiles, wall paints, insulating pads, etc.) to more obscure sources such as disk drive operations.[59] The most reliable method, albeit not necessarily the most cost-effective alternative, is to use chemical filters to manage AMC problems of both organic and inorganic natures.

While suppression of oAMCs has been successfully demonstrated through both air monitoring and device characterization,[60,61] meager information on the research and development of chemical filters is available, possibly due to its high proprietary and commercial values. In principle, chemical filters in cleanroom applications must be capable of dealing with high volumetric flow and low outgassing from filter materials themselves. Chemical filters targeting inorganic AMCs such as ammonia, sulfur dioxide, nitrogen dioxide, hydrochloric and hydrofluoric acids, have been relatively well developed. Conventionally, activated carbon in granular or fibrous structure has been used as the base material and adsorbent. To promote gas absorption, the porous activated carbons are frequently impregnated with either phosphoric (or citric) acid for the absorption of basic gases, or potassium permanganate (or hydroxide) for the absorption of acidic gases. Ionic exchange beads have also been impregnated into the supporting materials to capture ionic gas components and have been demonstrated to achieve better initial removal efficiency as well as prolonged breakthrough times for ammonia than chemical filters with chemical absorption.[62] Both chemical absorption and ion exchange are highly selective with respect to the target contaminant, and are sometimes limited in point-of-use applications such as the FFUs and filter-integrated process tools.

Control of organic compounds through van der Waals adsorption (i.e., physisorption) is difficult because of the presence of organic contaminants in trace concentration levels. As a result, the lack of concentration gradient, the drive force of pore diffusion, renders physisorption less effective. Chemical adsorption, typically impregnated onto the surface and into the pore structure of the base media, fills this deficiency by reacting with the organic (and inorganic) contaminants to bind them to the media surface. One example is delineated by Shiratori and co-workers,[63,64] who fabricated a "layer-by-layer self-assembly film" by chemically depositing poly(allylamine hydrochloride) (PAH) and poly(acrylic acid) (PAA) onto fiber glasses in sequence. Contaminants passing through the filter are adsorbed by the films due to Coulombic force and react with the polymers. They reported that the adsorption of acetyldehyde by PAH was four times more than activated carbon on an equivalent-weight basis. In addition, the removal efficiencies improved with the number of layers in the filter. Results from the infrared spectroscopic analysis confirmed that ammonia gas reacted with the carbonyl groups in PAA (Eq. 14a) and acetyldehyde gas reacted with the amine groups in PAH (Eq. 14b)

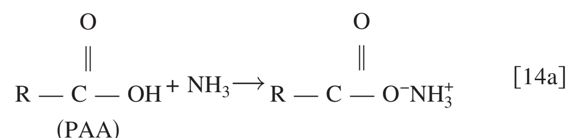

[14a]

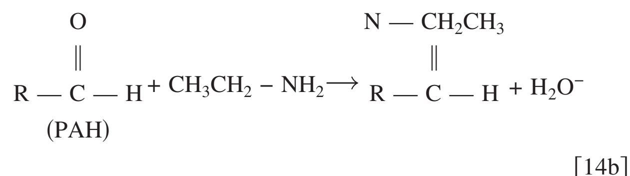

[14b]

Besides the development of sorption media, the filter configuration and materials are also gaining attention. For example, commercially available filter types include configurations such as honeycomb panel, flat panel with serpentine shape, and V-bank filter. All of these designs are to prolong the contact time and to increase the contact surface area between the media and gas. Furthermore, a number of carbonaceous (e.g., carbon fiber), noncarbonaceous (e.g., glass fiber, ceramic paper, nonwovens), and polymeric materials has been used as the blank filter. Horiuchi and Kouso[65] have compared the removal efficiency of benzene gases (30 ppmv) between a polyurethane (PU) foam-based and a polyethyleneterephthalate (PET)-based chemical filter, both coated with activated carbon. The initial benzene removal efficiency was 96% for the PET filter as compared to only 86% for the PU filter. The breakthrough curves obtained for a face velocity of $0.3\ m\ s^{-1}$ and a cross-sectional area of approximately $285\ mm^2$ also showed that at 80% removal efficiency, the PET filter (90 min) lasted significantly longer than the PU filter (50 min). Electron microscopic observation revealed that the nominal diameter of PET fiber ($50\ \mu m$) was nearly half that of the PU fiber, leading to much greater contact area for adsorption. Recently, photocatalytic screens have also been applied to complement chemi-

Downloaded on 2014-04-26 to IP 140.113.38.11 address. Redistribution subject to ECS terms of use (see ecsdl.org/site/terms_use) unless CC License in place (see abstract).

cal filters. This added unit, typically coated on woven cloth, could predecompose the organic contaminants into lower concentrations and smaller molecules for the subsequent adsorption by chemical filters. Vendors have reported, at face velocity of 0.5 m s^{-1} with test compounds of DEP (0.05–0.1 μg m^{-3}) and DBP (0.1–0.5 μg m^{-3}), the breakthrough time for 50% removal efficiency could be extended to 30 days with one-lamp illumination and longer than 70 days for three-lamp illumination.[66] The operating cost, however, may be as much as 20 times greater than conventional chemical filters. Therefore, the cost-effectiveness must be evaluated between the operating and equipment costs.

Conclusions

A review of the deposition of organic condensable molecular contaminants on silicon wafer surfaces in semiconductor device fabrication cleanrooms was performed. Problems associated with the airborne molecular contamination have gained increasing recognition, especially as the critical feature of circuit patterns falls below 100 nm. Although the ITRS has implemented threshold contamination levels for both organic and inorganic AMC in the technological roadmap for future device generations, these values are primarily derived from the observation of defect densities based on a limited number of case studies. It was only a few years ago that researchers devoted studies designed to evaluate the sources of outgassing and the deposition behaviors of the AMCs, particularly those of organic nature. It has been clarified that depending on the surface preparation of the wafer and the exposure duration, different groups of organic AMC could be detected from the wafer surfaces. In general, organic compounds with smaller molecular weight or higher vapor pressure tend to occupy wafer surfaces during initial exposure, but those with larger molecular weight gain the competitive advantage for adsorption in longer exposure times. A typical example is the predominance of DOP, a compound that does not naturally desorb from wafer surfaces, replacing smaller compounds pre-existing on the wafers.

Kinetic models ranging from simple first-order adsorption and desorption to more sophisticated multicomponent systems (MOSAIC) were discussed. The Langmuir kinetic model using DBP as a model contaminant satisfactorily described the longer term surface density collected from literature data with various ambient DBP concentrations. However, models such as MOSAIC must be applied to predict the concentration evolution of competing organic AMCs. The other parameter which is critical to the deposition kinetics is surface capacity. Theoretical values of the maximum molecular density could be calculated by estimating the molecular size of the targeting contaminant through van der Waals volume increments or molecular mechanics. The published data often varied by a wide margin of difference but are all below the theoretical value. The state of surface topography and defects was reported to greatly influence the number and types of adsorption sites available for molecular deposition.

A number of control strategies have been proposed to minimize the effects of molecular contamination. Implementation of chemical filters, which can be introduced at local processing or fab-scale environments, has become a necessity. Development of chemical filters has been vigorous due to its growing sales market; however, nonproprietary information is extremely limited. Nevertheless, it is clear that integration of physico- and chemicosorption by carbon adsorption, chemical absorption, and/or ion exchange mechanisms is the trend of product development, along with the stringent requirements of low outgassing and low pressure drops at high volumetric flow.

Tunghai University assisted in meeting the publication costs of this article.

References

1. S. A. MacDonald, W. D. Hinsberg, H. R. Wendt, N. J. Clecak, and C. G. Willson, *Chem. Mater.*, **5**, 346 (1993).
2. W. D. Hinsberg, S. A. MacDonald, and N. J. Clecak, *Chem. Mater.*, **6**, 481 (1994).
3. F. Matsuoka, in *Proceedings of the SEMI Technology Symposium*, Mountain View, CA, p. 6-3–6-9 (1999).
4. O. Kishkovich, D. A. Kinkead, J. Higley, R. Kerwin, and J. Piatt, *Proc. SPIE*, **1999**, 348.
5. S. J. Lue, T. Wu, H. Hsu, and C. Huang, *J. Chromatogr., A*, **804**, 273 (1998).
6. S. J. Lue, T. Wu, H. Hsu, and C. Huang, *J. Chromatogr., A*, **850**, 283 (1999).
7. A. J. Muller, L. A. Psota-Kelty, H. W. Krautter, and J. D. Sinclair, *Solid State Technol.*, **37**, 61 (1994).
8. J. A. Lebens, W. C. McColgin, and J. B. Russell, *J. Electrochem. Soc.*, **143**, 2906 (1996).
9. H. Bai, Y. Kang, and C. Liu, *Aerosol & Air Quality Res.*, **2**, 53 (2002).
10. S. R. Kasi and M. Liehr, *J. Vac. Sci. Technol. A*, **10**, 795 (1992).
11. K. J. Budde, W. J. Holzapfel, and M. M. Beyer, *J. Electrochem. Soc.*, **142**, 888 (1995).
12. M. Tamaoki, K. Nishiki, A. Shimizaki, Y. Sasaki, and S. Yanagi, in *Proceedings of the IEEE/SEMI Advanced Semiconductor Manufacturing Conference*, Cambridge, MA, p. 322 (1995).
13. T. Ogata, C. Ban, A. Ueyama, S. Muranaka, T. Hayashi, K. Kobayashi, J. Kobayashi, H. Kurokawa, Y. Ohno, and M. Hirayama, *Jpn. J. Appl. Phys., Part 1*, **37**, 2468 (1998).
14. N. B. Rana, P. Raghu, and F. Shadman, *J. Electrochem. Soc.*, **145**, F35 (2002).
15. N. B. Rana and F. Shadman, *IEEE Trans. Semicond. Manuf.*, **16**, 76 (2003).
16. N. B. Rana, P. Raghu, E. Sharo, and F. Shadman, *Appl. Surf. Sci.*, **205**, 160 (2003).
17. H. Kitajima and Y. Shiramizu, *IEEE Trans. Semicond. Manuf.*, **10**, 267 (1997).
18. SEMI Standard F21-95, Semiconductor Equipment and Materials International, Mountain View, CA (1996).
19. C. Muller, *J. IEST*, **42**, 19 (1999).
20. C. Muller, *Semicond. Fabtech*, **16**, 113 (2002).
21. S. M. Thornburg, D. C. McIntyre, A. Y. Liang, S. F. Bender, and R. D. Lujan, Technology Transfer Report 9402208A-XFR, Sematech (1994).
22. P. Aragon, J. Atienza, and M. D. Climent, *Crit. Rev. Anal. Chem.*, **30**, 121 (2000).
23. T. Otake, J. Yoshinaga, and Y. Yanagishiwa, *Environ. Sci. Technol.*, **35**, 3099 (2001).
24. H. Toda, K. Sako, Y. Yagome, and T. Nakamura, *Anal. Chim. Acta*, **519**, 213 (2004).
25. P. A. Clausen, V. Hansen, L. Gunnarsen, A. Afshari, and P. Wolkoff, *Environ. Sci. Technol.*, **38**, 2531 (2004).
26. A. R. Mastrogiacomo, E. Pierini, and L. Sampaolo, *Chromatographia*, **41**, 599 (1995).
27. Y. Kang, W. Den, H. Bai, and F.-H. Ko, *J. Chromatogr. A* **107**, 137 (2005).
28. A. Licciardello, O. Puglisi, and S. Pignataro, *Appl. Phys. Lett.*, **48**, 41 (1986).
29. T. Takahagi, I. Nagai, A. Ishitani, H. Kuroda, and Y. Nagasawa, *J. Appl. Phys.*, **64**, 3516 (1988).
30. G. G. Goodman, P. M. Lindley, and L. A. McCaig, *Semicond. Fabtech*, **13**, 131 (2001).
31. P. A. Clausen and P. Wolkoff, *J. High Resolut. Chromatogr.*, **20**, 99 (1997).
32. ASTM F1982-99, American Society for Testing and Materials; This standard was transferred to SEMI on May 2003, and withdrawn from ASTM standards.
33. IEST-RP-CC031, Institute of Environmental Sciences and Technology (2004).
34. SEMI-E108-0301, SEMI Environmental Contamination Control (2002).
35. F. Sugimoto and S. Okamura, *J. Electrochem. Soc.*, **146**, 2725 (1999).
36. Y. Kang, W. Den, H. Bai, and F.-H. Ko, *J. IEST*, **48**, 21 (2005).
37. C. Inoue, N. Mizuno, S. Ogura, Y. Hanayama, S. Hattori, K. Endo, K. Yasutake, M. Morita, and Y. Mori, *J. Inst. Environ. Sci. Technol.*, **44**, 23 (2001).
38. K. Takeda, A. Mochizuki, T. Nonaka, I. Matsumoto, T. Fujimoto, and T. Nakahara, *J. Inst. Environ. Sci. Technol.*, **44**, 28 (2001).
39. K. Saga and T. Hattori, *J. Electrochem. Soc.*, **143**, 3279 (1996).
40. D. Hou, P. Sun, M. Adams, T. Hedges, and S. Govan, in *Proceedings of 44th Annual Technical Meeting, Institute of Environmental Sciences and Technology*, Phoenix, AZ, p. 419 (1998).
41. Y. Ishihara, D. Nakajima, and T. Ohmi, *IEEE Trans. Semicond. Manuf.*, **13**, 16 (2000).
42. R. Genco, J. Pitts, and G. Galleger, *Semicond. Int.*, **4**, 91 (1997).
43. J. Frickinger, J. Bugler, G. Zielonka, L. Pfizner, H. Ryssel, S. Hollemann, and H. Schneider, *IEEE Trans. Semicond. Manuf.*, **13**, 427 (2000).
44. M. Veillerot, A. Danel, S. Marthon, and F. Tardif, *Solid State Phenom.*, **92**, 105 (2003).
45. S.-B. Zhu, *J. IEST*, **41**(4), 30 (1998).
46. S.-B. Zhu, *J. IEST*, **41**(5), 36 (1998).
47. T. Takahagi, S. Shingubara, H. Sakaue, K. Hoshino, and H. Yashima, *Jpn. J. Appl. Phys.* **35**, L818 (1996).
48. H. Habuka, M. Shimada, and K. Okuyama, *J. Electrochem. Soc.*, **147**, 2319 (2000).
49. H. Habuka, M. Shimada, and K. Okuyama, *J. Electrochem. Soc.*, **148**, G365 (2001).
50. S. Ishiwari, H. Kato, and H. Habuka, *J. Electrochem. Soc.*, **148**, G644 (2001).
51. J. T. Edward, *J. Chem. Educ.*, **47**, 261 (1970).
52. Y. Kiso, T. Kon, T. Kitao, and K. Nishimura, *J. Membr. Sci.*, **182**, 205 (2001).
53. H. Habuka, S. Ishiwari, H. Kato, M. Shimada, and K. Okuyama, *J. Electrochem. Soc.*, **150**, G148 (2003).
54. S. Okamura, M. Shimada, and K. Okuyama, *Jpn. J. Appl. Phys., Part 1*, **43**, 2661 (2004).
55. S. Okamura, M. Shimada, and K. Okuyama, *Jpn. J. Appl. Phys., Part 1*, **43**, 5496 (2004).
56. D. A. Kinhead, Technology Transfer Report 95052812A-TR, Sematech (1995).
57. M. Veillerot, A. Danel, S. Cetre, and F. Tardif, *Mater. Sci. Eng., B*, **102**, 385 (2003).

Downloaded on 2014-04-26 to IP 140.113.38.11 address. Redistribution subject to ECS terms of use (see ecsdl.org/site/terms_use) unless CC License in place (see abstract).

58. M. Saito, in *International Symposium on IEEE/UCS/SEMI*, Austin, TX, p. 171 (1995).
59. D. E. Fowler, R. Duque, T. Anoikin, and J. Zhou, *IEEE Trans. Semicond. Manuf.*, **39**, 769 (2003).
60. C.-F. Yeh, C.-W. Hsiao, S.-J. Lin, C.-M. Hsieh, T. Kusumi, H. Aomi, H. Kaneko, B.-T. Dai, and M.-S. Tsai, *IEEE Trans. Semicond. Manuf.*, **17**, 214 (2004).
61. C.-W. Hsiao, J.-C. Lou, C.-F. Yeh, C.-M. Hsieh, S.-J. Lin, and T. Kusumi, *Jpn. J. Appl. Phys., Part 2*, **43**, L659 (2004).
62. K. Horiuchi, J. Shibata, and D. Kouso, *J. Appl. Polym. Sci.*, **78**, 1312 (2000).
63. S. Shiratori, T. Suzuki, S. Kushida, and Y. Inami, *Sens. Mater.*, **13**, 77 (2001).
64. S. Shiratori, Y. Inami, and M. Kikuchi, *Thin Solid Films*, **303**, 243 (2001).
65. K. Horiuchi and D. Kouso, *Mater. Lett.*, **57**, 2352 (2003).
66. Nippon Muki Co., Ltd., Personal communication.
67. Sematech International, International Technology Roadmap for Semiconductors (ITRS), Austin, TX (2003).
68. Y. Kang, Ph.D. Dissertation, National Chiao-Tung University, Hsinchu, Taiwan (2005).
69. R. Sasajima, E. Takami, N. Nakamura, and H. Miya, in *Proceedings of the 19th Annual Technical Meeting on Air Cleaning and Contamination Control*, Tokyo, Japan, p. 10 (2002) [in Japanese].
70. K. Takeda, T. Nonaka, Y. Sakamoto, T. Taira, K. Hirono, T. Fujimoto, N. Suwa, and K. Otsuka, in *Proceedings of the Institute of Environmental Sciences and Technology*, Phoenix, AZ, p. 556 (1998).
71. Y. Sakamoto, K. Takeda, T. Taira, T. Nonaka, K. Hirono, T. Fujimoto, N. Suwa, and K. Otsuka, in *Proceedings of the 16th Annual Technical Meeting on Air Cleaning and Contamination Control*, Tokyo, Japan, p. 215 (1998) [in Japanese].
72. H. Takahashi, K. Sato, S. Sakata, and T. Okada, in *Proceedings of the 16th Annual Technical Meeting on Air Cleaning and Contamination Control*, Tokyo, Japan, p. 231 (1998) [in Japanese].
73. T. Takatsuka, M. Tomonari, M. Godo, K. Miura, H. Sata, K. Yajima, S. Takami, M. Kubo, and A. Miyamoto, in *Proceedings of the 19th Annual Technical Meeting on Air Cleaning and Contamination Control*, Tokyo, Japan, p. 5 (2001) [in Japanese].

Downloaded on 2014-04-26 to IP 140.113.38.11 address. Redistribution subject to ECS terms of use (see ecsdl.org/site/terms_use) unless CC License in place (see abstract).